Available online at www.sciencedirect.com

ScienceDirect

Procedia CIRP 00 (2025) 000–000

www.elsevier.com/locate/procedia

20th CIRP Conference on Modeling of Machining Operations

On machine 3D reconstruction of endmill tool wear

Joseph Betts[a]*, Shamin Sadrafshari[a], Ali Mohammadi[a], Alborz Shokrani[a]

[a]*University of Bath, Bath, BA2 7AY, United Kingdom*

* Corresponding author. Tel.: +441225 38 6588. *E-mail address:* jtb32@bath.ac.uk

Abstract

During the machining of difficult-to-machine materials, monitoring the tool wear is essential to avoid excessive wear negatively impacting the part's surface integrity or damaging the part beyond repair. When manually monitoring the tool wear, the machine operator must physically remove the tool from the machine at regular intervals to inspect the tool wear, which can be very time-consuming. Instead, tools are often changed when the wear is significantly below the maximum allowable value, adding to the part production cost, environmental impact and machine downtime. This paper presents a method for in-situ tool wear measurement using a laser line scanner placed inside a machine tool, providing a 3-D model of the tool in its current condition. This can be performed without operator intervention and the 3-D reconstruction of the tool can then be used for further analysis. The proposed method can provide an automated system for generating tool wear database for training machine learning models. Additionally, it can be combined with machine learning-based indirect tool condition monitoring (TCM) methods, allowing the models to self-validate predicted tool wear values, further reducing operator input and increasing productivity.

Keywords: Cutting Tools; Tool Condition Monitoring; Machining

1. Introduction

During the machining process, tool wear and subsequent tool failure are problems that commonly occur and are critical factors affecting both the surface integrity of the workpiece and production cost. Increased tool wear can result in poor surface integrity [1], and high cutting forces [2] and vibrations [3], ultimately leading to tool failure. If the tool failure occurs during a machining operation, it can lead to scrapping of the part, which can incur a significant cost and waste production. To avoid these issues, it is common in the industry to change the tool significantly before the failure point as actual tool wear values are often not measured and failure during machining is deemed unacceptable. This not only adds additional cost to the production of the part but, also increases the environmental impacts of machining processes which is an area of increasing concern [4].

There are several methods for Tool Condition Monitoring (TCM) during machining, these can be broadly split into direct and indirect monitoring techniques [5]. The simplest of these is direct monitoring [6] where physical measurements are taken of the tool wear at discrete intervals. Due to the nature of the machining operations, the cutting edge of the tool is mostly inaccessible. Hence, direct methods typically involve stopping the cutting process to take tool wear measurements between machining passes. The most common direct measurement technique used in research is optical imaging. This consists of removing the tool from the machine, taking an image, and returning the tool to continue machining. Due to the required downtime, this method has few applications in a production environment. There have been several attempts to automate this process and reduce operator intervention. Ruitao et al. [7] employed an on-machine camera constantly pointing at the tool to take flank wear images between passes and process them using machine vision. A similar machine vision approach was used by Yu et al. [8] to record wear on the underside of drill bits during the machining process. These have shown success in automated recording of a single wear type but to gain a full picture of rake and flank wear on an endmill, a more complicated multicamera setup would be required. The most recent research on direct monitoring of tool wear has been done using a laser line scanner. Čerče et al. [9] developed a system to generate a 3D scan of a turning insert. This initial measurement system required the removal of the insert from the machine before scanning. They later went on to develop a system to generate the same scan from within a CNC lathe [10] providing an accurate reconstruction of the insert without removing it from the machine.

An alternative method of TCM is indirect monitoring. With the increasing use of machine learning within manufacturing, there has been a significant amount of research dedicated to indirect TCM. This is a continuous process where sensor readings such as cutting forces and vibrations are recorded during the machining operation and correlated to the tool wear state. This has the advantage over direct monitoring in that the machining operation does not need to be paused to assess the tool wear. Additionally, the constant monitoring means that the process can be stopped if the system predicts the tool is about to fail. A large variety of sensors have been used for this process including accelerometers [11], cutting force/bending moment data [12], power and acoustic emission data [13]. These methods have the capability to accurately predict tool wear. However, they still rely on initial direct measurements to generate a training dataset. Additionally, to validate the models, periodic direct measurements should be taken to assess their performance.

To allow for both an improved direct monitoring method of TCM during the milling process, and to propose a method by which indirect TCM systems can be trained and validated, this study will focus on the methodology for generating a 3D reconstruction of an end mill tool with the focus of viewing flank and rake wear. This will be designed to take place within the machine tool, with minimal set-up requirements allowing for rapid and accurate tool wear measurements to be captured, reducing the downtime in machining operations without sacrificing the accuracy of the measurements.

Nomenclature

CNC	Computer Numerical Control
CPD	Coherent Point Drift
FGR	Fast Global Registration
FPFH	Fast Point Feature Histogram
IPC	Iterative Close Point
NDT	Normal Distribution Transformation
TCM	Tool Condition Monitoring

2. Measurement system

2.1. Measurement system hardware

For this research, a new measurement system has been developed to allow a full 3D reconstruction of an endmill tool on the machine. This enables tool wear measurements to be taken without removing the tool from the machine, reducing machine downtime and increasing productivity. The measurement setup can be seen in Figure 1.

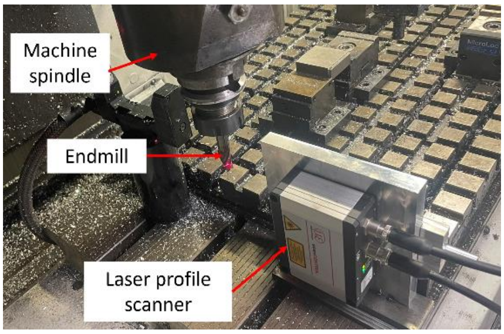

Figure 1. Measurement system installed in Bridgeport VMC 610xp machine tool.

This setup incorporates a Micro Epsilon scanCONTROL 30x2 high-performance laser line scanner placed inside the machine tool outside of the typical machine area utilised for machining. The details of this laser line scanner can be found in Table 1.

Table 1. Details of Micro Epsilon Laser Scanner.

Model Number	scanCONTROL 30x2
Sensor Resolution	1024 points/scan
Point Distance	24 µm
Measurement Range	25 x 25 mm
Maximum profile frequency	2 kHz
Lase Bandwidth	658 nm
Laser Colour	Red

Having the scanning system in the machine enables the CNC machine axis to be used for motion during the tool scanning process, reducing the need for additional equipment/control systems. It also allows the tool scanning to be programmed into the G-code reducing the need for operator input for on-machine tool condition monitoring. The laser line scanner was connected to a computer running scanCONTROL 3D-View using the built-in ethernet connection. scanCONTROL 3D-View is first-party software from Micro Epsilon, used to adjust the measurement parameters, capture the 3D data and export the captured data as a 3D point cloud for further processing. A schematic of the measurement system can be seen in Figure 2. Details of the MATLAB [14] processing carried out on the point cloud scans will be detailed below.

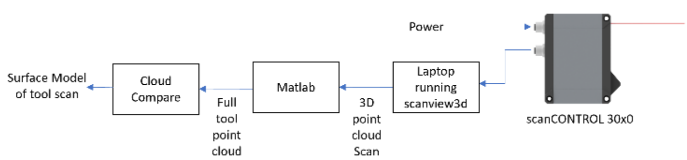

Figure 2: Measurement system schematic of 3D tool scan process.

Following the MATLAB processing of the scanned point clouds, the full tool point cloud model is exported and imported into CloudCompare [15] for surface reconstruction. The normals of the point cloud are calculated, orientated using minimum spanning tree, and then a surface is reconstructed using the PoissonRecon [16] plugin based on the work by Kazhdan et al. [17]. The surface reconstruction is carried out to enable better visualisation of the scanned surface and any defects that are present.

The laser line scanner operates by outputting a series of laser points and triangulating the distance between the point reflection and the sensor head. As the surface of cutting tools is commonly reflective, selecting the appropriate sensor setting is critical to ensure that the profile is recorded accurately without erroneous reflections being recorded. Figure 3 shows the results of a scan with incorrect settings next to a scan with the settings adjusted.

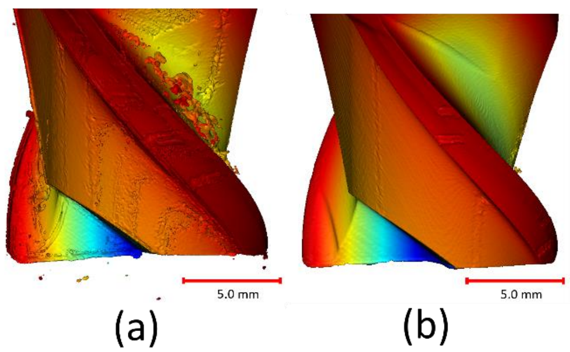

Figure 3. Initial 3D scans of tools with (a) initial laser scanner configuration settings, (b) with settings adjusted to minimise reflections.

The settings of the laser scanner were varied until accurate clear scans could be recorded. The final settings used during the work are given in Table 2.

Table 2. Laser line scanner configuration.

Sensor Setting	Selected Value
Exposure Time (ms)	1
Scanning Frequency (Hz)	650
Laser Power	Standard
Sensitivity	High
Reflections	Highest Intensity
Reflection threshold (%)	75

With the initial laser configuration set to allow scanning with minimal reflection artefacts, the scanning methodology was now developed to allow for 3D tool reconstruction.

2.2. Tool scanning methodology

To scan the tool, the direction of scanning needed to be selected. For this research, the tool was kept in a fixed rotation during each scanning pass, with the scanning being carried out in the vertical directions. For this to be possible, the laser scanner beam was orientated perpendicular to the tool rotation axis, see Figure 4 (a).

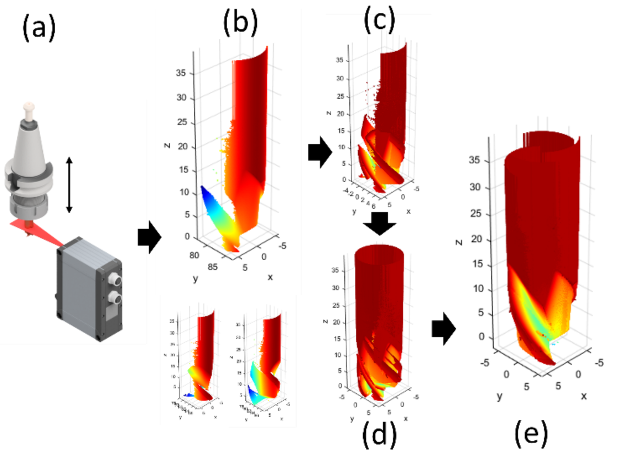

Figure 4. Scanning strategy for 3D reconstruction of the static tool.

The scanning process for the static tool is as follows:

1) The tool moves to just about the laser scanner inside of the machine tool.
2) The laser line scanner starts recording and the tool is moved down along the Z-axis until the full cutting area is scanned.
3) The tool returns to the initial Z position and rotates a specific amount whilst the captured point cloud is exported.
4) Steps 2 and 3 are repeated until the full 360° of the tool is captured.
5) The exported 3D point cloud scans are then imported into MATLAB and subsequently CloudCompare for processing and registration whilst the tool returns to the working area and continues with machining.

With the scans imported into MATLAB, the following processing steps are performed to enable a full point cloud of the tool to be generated. The initial point clouds imported are all in the same position in 3D space as from the laser scanners' perspective, all of the scans were in the same location, Figure 4 (b). The initial processing step finds the centre of these imported point clouds using the top of the scan, where the tool shank was scanned and checks the calculated radius to ensure the scan is scaled correctly. Each scan is then translated to be centred about the origin of the XY plane, Figure 4 (c). The point clouds are then rotated around the z-axis to place them in the correct orientation rotationally as shown in Figure 4 (d). Finally, as demonstrated in Figure 4 (e), the point clouds are registered one at a time to fully align with each other.

The registration algorithm used in MATLAB to combine the point clouds was the fast global registration (FGR) algorithm from the Lidar toolbox [18]. This function registers point clouds using a fast global registration algorithm based on FPFH features. The process used by this algorithm is shown in Figure 5.

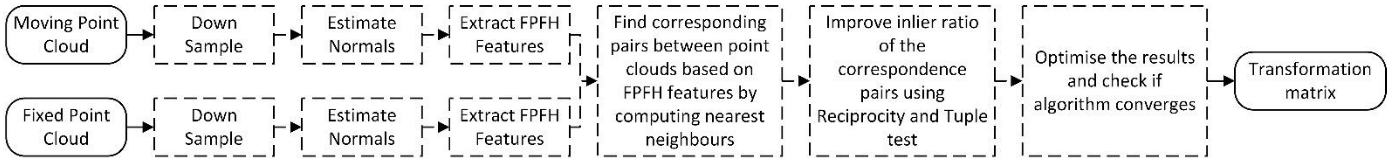

Figure 5. Process of point cloud registration using the pcregisterfgr function.

There are a number of other point cloud registration algorithms built into MATLAB and these were also tested to assess their performance. The four main alternatives are the pcregistericp, pcregistercpd, pcregisterndt and pcregistercorr which use iterative closest point (ICP), coherent point drift (CPD), normal-distributions transform (NDT) and an image-based phase correlation algorithm respectively, to align the point clouds. The results of these algorithms along with the time taken to complete the full registration of 6-point cloud tool scans are shown in Figure 6. For this comparison, the parameters for registration for each algorithm have been adjusted to give a comparable registration time to the FGR algorithm.

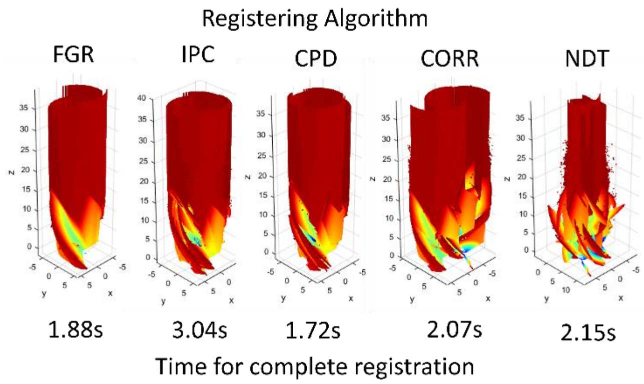

Figure 6. Comparison of completed point cloud registrations with different registration algorithms.

Figure 6 shows that FGR registration provided the best registration in a short amount of time and hence was selected for further investigation in this study.

As the laser line scanner accurately records the profile of the tool in the x and y direction to ensure a fully accurate scan the value of the z position for each scan needs to be recorded. To do this an accurate federate in the z axis of 600 mm/min was programmed into the Siemens 840d pl controller of the machine tool that was used in this research. The tool's initial position was also set high enough above the start of the sensor for recording to ensure that the tool had accelerated to the set federate before the recording had started. The precise angle for each scan was also programmed using the machine controller allowing for accurate and repeatable scans to be made. This 600 mm/min feed rate was converted to 10 mm/s which was entered into the scanCONTROL 3D view software where along with the known 650 Hz recording rate the distance between each line scan was calculated.

3. 3D tool reconstruction

To determine the effectiveness of the tool scanning methodology scans of a new and worn tool were taken of a four-flute tungsten carbide endmill with a TiSiN coating. The tool material should not have any impact on the effectiveness of the scanning for future work. However, as the process relies on the reflection of the laser point on the tool surface, different coatings or differences in the tool reflectivity may result in degraded performance and require the laser line scanner settings in Table 2 to be adjusted. Before scanning, the tools were cleaned with isopropyl alcohol to remove any surface contamination from the coolants used during their life. For the further development of this process for on-machine monitoring of tool wear during machining experiments, a system will need to be developed to remove any coolants/swarf stuck to the tool's surface and to dry it before scanning, possibly with an air blast.

The areas that are of primary focus for monitoring the wear on a tool are the rake and flank faces. To assess the performance of the 3D scanning system, images of the new and worn tools were taken on a Keyence VHX 6000 digital optical microscope with 50× magnification for comparison. These are representative images of the current processes carried out for microscope-based tool wear measurements during the milling process [19, 20]. Figure 7 shows images of the rake and flank faces of the new tools.

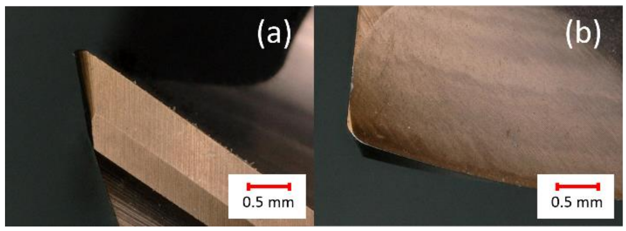

Figure 7. Microscope images of a new tool (a) flank and (b) rake faces.

3D scans of the tools were then taken following the method detailed above. For the following tool scans, the feed rate in the z-axis used for scanning was 600 mm/min with 2500 scans being required to perform a single scan of the tool surface. At the sampling frequency of 650 Hz, this means that the time for a single scan of the tool's surface is 3.8 s. The tool scans presented below were generated using 12 scans of the tools with a rotation of 30° between each scan. This means that the time required for a machining operation to be paused to capture tool wear data is 45.6 seconds. This time could be reduced by reducing the resolution of the scan in the Z-direction, increasing the feed rate, or reducing the number of scans per tool. With a tool with a smaller number of flutes, a lower number of scans will be required to generate the full tool reconstruction.

Figure 8 shows the initial scans of the new tools. In this Figure, it can be seen that the proposed methodology and equipment used can accurately generate a 3D model of the tool.

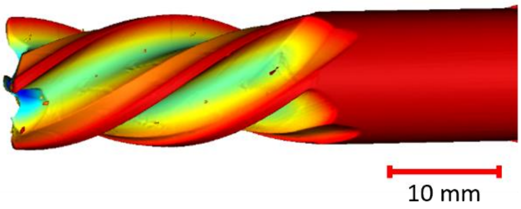

Figure 8. Full tool 3D reconstructions of a four-flute endmill.

To further access the detail of the scan, the rake and flank faces of the 3D tool reconstructions were inspected. Images of the rake and flank faces of the tool reconstruction can be seen in Figure 9.

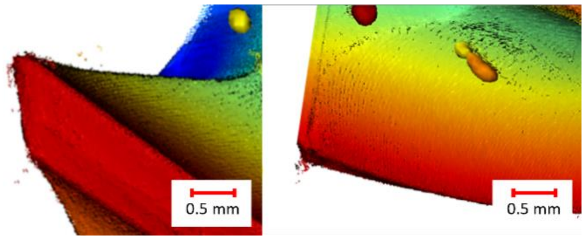

Figure 9. Images of the new tool (a) flank and (b) rake faces taken from the 3D reconstruction.

In Figure 9, it can be seen that the images of the rake and flank faced look very similar to the images in Figure 7 indicating that the scanning methodology proposed above can accurately capture information of the tool geometry in the key areas that are relevant to tool wear. A similar procedure was repeated with a worn tool with known flank wear. Figure 10 shows a comparison of the wear on a single flute rake and flank faces between the tool wear images and the 3D reconstruction.

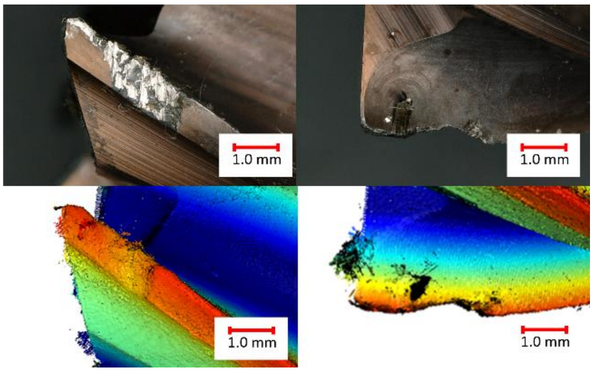

Figure 10. Comparison of rake and flank wear images from microscope imaging and 3D reconstruction.

As can be seen in Figure 10, the 3D tool reconstruction is able to capture both the wear on the rake and flank faces and give comparable detail to tool wear images. The 3D reconstruction has the benefit of being able to provide details of both the rake and flank faces from a single scan. In addition to this, as well as allowing the typical wear measurements of the flank face following ISO 8688-1, it also provides depth information to these images allowing for identification of workpiece adhesion to the tool and build-up edge to be quantified in addition to being imaged.

To ascertain the accuracy of tool flank wear measurements for the 3D reconstruction, compared to the conventional optical methods, images of the four tool flank faces for both methods were imported into the BRESSER MikroCamLabII software. The software scale was then calibrated according to the scale bars on the image and tool flank wear values were manually measured. The average flank wear for the optical images was 775.4 ± 20.6 µm and for the 3D tool reconstructions was 773.6 ± 28.6 µm. This indicates that not only can images of the tool be recreated through the 3D tool scan, the tool wear values can also be accurately captured within the limits of manual tool wear measurement.

The only difficulty with these images is that the 3D model does not contain the colour information from the original tool making identifying the actual flank wear from this view alone difficult. In the future, the measurement system could be modified to capture the image data and combine it with the 3D reconstruction giving the best of both methods.

A final process that can be carried out is to ‘unfold’ the 3D scan of the tool around the Z-axis. This allows the reconstruction of the tool to be viewed all at once making it particularly easy to view the flank face of the tool. This means that the wear on all teeth of a cutting tool can be assessed at once without the need for manipulating the 3D tool model. Figure 11 shows the unfolded image of the new tool and Figure 12 the worn tool.

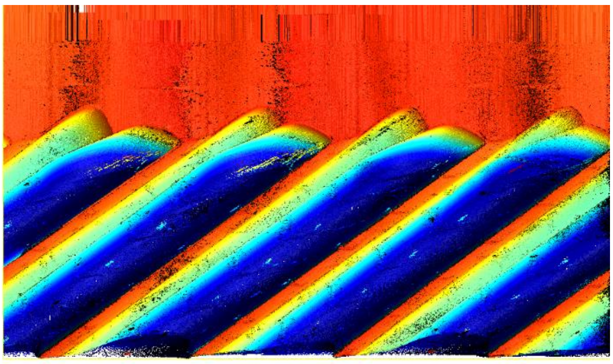

Figure 11. 3D reconstruction of a new tool unfolded around the z-axis to allow better visibility of the whole tool condition.

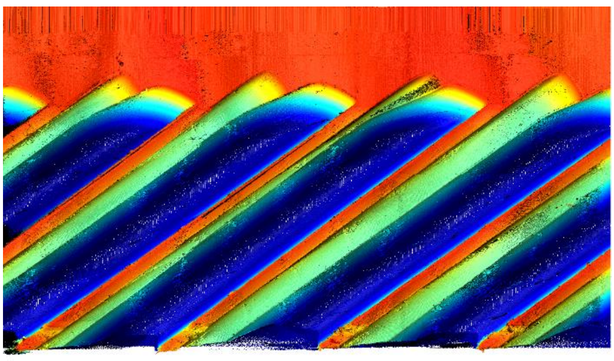

Figure 12. 3D reconstruction of a worn tool unfolded around the z-axis to allow better visibility of the whole tool condition.

4. Conclusions and future work

In this study, a measurement system and methodology were developed for on-machine 3D reconstruction of rotating tools typically used in milling operations. It was tested for the scanning of a new and worn endmill for tool wear monitoring on a vertical milling centre. It was found that the system was fully capable of capturing the geometry of an endmill through several scans with the tool static utilising the Z motion of the spindle to scan the tool.

In both cases of new and worn tools, the 3D reconstruction allowed similar images to be generated that would conventionally be taken in offline tool wear monitoring using a digital microscope. Images of the 3D tool reconstruction were compared to microscope images of the same tool and were found to provide comparable images when viewed from the same angle. The 3D reconstruction outperforms conventional methods as it allows the same tool wear measurements to be taken and provides additional depth information allowing the identification of adhesion of workpiece material to the tool and identification of built-up edge.

Another advantage of the 3D reconstruction over conventional imaging is, the machining process only had to be stopped for 45.6s, to allow the scans to take place, with the tool measurements being able to be taken once the machining operation has continued. This offers a significant reduction in machine downtime compared to conventional methods of tool wear measurement which require the operator to physically remove the tool from the machine to take the measurements. This proposed method of tool wear reconstruction also reduces the operator burden as the entire measurement process can be automated and programmed into the machine tool controller.

The proposed method therefore provides a promising method for automated direct tool wear measurement which offers several benefits over conventional optical tool wear measurement. Future work will focus on fully automating the system including the wear measurements to allow a hands-off method for tool condition monitoring. This could then be linked to predictive machine learning models to allow the machining process to be monitored, adjusted and stopped dependent on the tool wear level. This would maximise the tool life, reduce the need to prematurely change the tool and reduce the likelihood of unacceptable damage to the workpiece surface.

As the tools scanned during this paper were manually cleaned prior to scanning, to allow the fully automated tool wear measurement to take place an air blade/air blast system will need to be implemented immediately prior to scanning. This will clean and dry the tool just before it passes in front of the laser line, allowing accurate scanning to take place without affecting the speed of the system.

Additionally, the measurement systems can be modified to further improve the speed and reliability of the data capture. This could be through testing of feeds and capture frequencies to determine the minimum resolution needed for full tool reconstruction or through testing alternate measurement methods.

Acknowledgements

The authors acknowledge the support from the United Kingdom Engineering and Physical Sciences Council for the SENSYCUT project under the grant number: EP/V055011/1.

References

1. Gupta, M.K., et al., Comparison of Tool Wear, Surface Morphology, Specific Cutting Energy and Cutting Temperature in Machining of Titanium Alloys Under Hybrid and Green Cooling Strategies. International Journal of Precision Engineering and Manufacturing-Green Technology, 2023. **10**(6): p. 1393-1406.
2. Zhang, G., J. Wang, and S. To, Tool Wear Monitoring Method Using Cutting Force in Ultra-precision Raster Milling, in Fly Cutting Technology for Ultra-precision Machining, S. To and S. Wang, Editors. 2023, Springer Nature Singapore: Singapore. p. 181-214.
3. Dimla, S.D.E., The Correlation of Vibration Signal Features to Cutting Tool Wear in a Metal Turning Operation. The International Journal of Advanced Manufacturing Technology, 2002. **19**(10): p. 705-713.
4. Shokrani, A., et al., Sustainable machining: Recent technological advances. CIRP Annals, 2024. **73**(2): p. 483-508.
5. Shokrani, A., et al., Sensors for in-process and on-machine monitoring of machining operations. CIRP Journal of Manufacturing Science and Technology, 2024. **51**: p. 263-292.
6. Ambhore, N., et al., Tool Condition Monitoring System: A Review. Materials Today: Proceedings, 2015. **2**(4): p. 3419-3428.
7. Ruitao, P., et al., Study of Tool Wear Monitoring Using Machine Vision. Automatic Control and Computer Sciences, 2020. **54**(3): p. 259-270.
8. Yu, J., et al., A machine vision method for measurement of machining tool wear. Measurement, 2021. **182**: p. 109683.
9. Čerče, L., F. Pušavec, and J. Kopač, 3D cutting tool-wear monitoring in the process. Journal of Mechanical Science and Technology, 2015. **29**(9): p. 3885-3895.
10. Cerce, L., F. Pusavec, and J. Kopac, Novel Spatial Cutting Tool-wear Measurement System Development and its Evaluation. Procedia CIRP, 2015. **37**: p. 170-175.
11. Hassan, M., A. Mohamed, and H. Attia, A Generalized Multi-Stage Deep Machine Learning Framework for Tool Wear Level Prediction in Milling Operations. Procedia CIRP, 2024. **126**: p. 441-446.
12. Hall, S., et al., ConvLSTM deep learning signal prediction for forecasting bending moment for tool condition monitoring. Procedia CIRP, 2022. **107**: p. 1071-1076.
13. Teti, R., et al., Process monitoring of machining. CIRP Annals, 2022. **71**(2): p. 529-552.
14. The MathWorks, I., MATLAB Version: 24.2.0.2740171 (R2024b). 2024.
15. CloudCompare. CloudCompare Version: 2.14 alpha. 2024; Available from: http://www.cloudcompare.org/.
16. CloudCompare. Poisson Surface Reconstruction (plugin). 2024; Available from: https://www.cloudcompare.org/doc/wiki/index.php/Poisson_Surface_Reconstruction_(plugin).
17. Kazhdan, M., M. Bolitho, and H. Hoppe. Poisson surface reconstruction. in Proceedings of the fourth Eurographics symposium on Geometry processing. 2006.
18. The MathWorks, I., Lidar Toolbox Version 24.2 (R2022b). 2024.
19. Wu, X., et al. Automatic Identification of Tool Wear Based on Convolutional Neural Network in Face Milling Process. Sensors, 2019. **19**, DOI: 10.3390/s19183817.
20. Shokrani, A., J. Betts, and I.S. Jawahir, Improved performance and surface integrity in finish machining of Inconel 718 with electrically charged tungsten disulphide MQL. CIRP Annals, 2022. **71**(1): p. 109-112.